Bull Volcanol (2009) 71:495–508
DOI 10.1007/s00445-008-0228-8

RESEARCH ARTICLE

Heterogeneous initial Sr isotope compositions of highly evolved volcanic rocks from the Main Ethiopian Rift, Ethiopia

Catherine Deniel

Received: 19 April 2007 / Accepted: 12 June 2008 / Published online: 23 August 2008

Abstract Many individual mineral Sr isotope studies have revealed the complex evolution of highly evolved rocks in upper crustal magmatic systems, casting doubts on the meaning of whole-rock Sr isotopes in such samples. In this paper, whole-rock Sr isotope measurements were replicated (three to 13 times) on six highly evolved peralkaline rhyolites from the Main Ethiopian Rift (MER) to appraise their internal heterogeneity and, thus, the significance of such data. These rocks were all fresh samples of pumice, obsidian and lava. Their maximum Sr contents and ages were 15 μg/g and 1.7 Ma, respectively. Significant small-scale heterogeneities of both Sr isotopes and Rb and Sr contents were observed in most samples, although not necessarily associated with petrological characteristics suggesting possible inheritance processes. Only two, almost crystal-free, obsidian give fairly homogeneous Sr isotope ratios. These results outline the ambiguity of a single whole-rock Sr isotope determination on highly evolved peralkaline rocks, especially when no simultaneous accurate determination of the Rb/Sr is performed. They also suggest that the limitations of Sr whole-rock analyses are not restricted to phenocryst-rich samples as phenocryst-poor obsidian and almost aphyric pumices and lava are also concerned. These data further underscore that unreplicated whole-rock Sr isotope measurements should always be used with great caution in the petrogenetic modeling of highly evolved rocks. However, multiple determinations of whole rock $^{87}Sr/^{86}Sr$ in the same samples, combined with other geochemical and isotopic data, may provide constraints on the shallow level evolution of these magmas. It is suggested that selective upper crustal contamination and/or interactions with halogen-bearing hydrous fluids, typical of evolved peralkaline magmas, were probably involved in the late magmatic evolution of these MER rhyolites. The more pervasive character of fluid interaction processes would probably better account for the small-scale association of uncontaminated and contaminated signatures in a single sample. Thus, even fresh samples may have their Rb–Sr isotopic system significantly modified by fluid interactions, not as a secondary process but at the late magmatic stage.

Keywords Sr isotopes · Heterogeneity · Highly evolved · Peralkaline · Volcanic rocks · Main Ethiopian Rift

Introduction

Sr isotope compositions have been largely used over the past 45 years, in addition to petrological, geochemical and some other isotope data to understand the petrogenesis of highly evolved magmas. In the oldest studies, only whole-rock Sr isotope ratios were available and considered as representative of the isotopic compositions of the liquids from which these rocks crystallized. It was assumed that for young, fresh volcanic rocks, mineral phases were in isotopic equilibrium with the host lava. However, petrological observations often reveal indices of crystals–liquid disequilibrium (mineral zoning, dissolution–resorption rims, overgrowth textures on resorbed crystals) suggesting a complex evolution of these magmas during their residence in magmatic systems.

Furthermore, various studies have outlined the Sr-isotope disequilibrium between feldspar phenocrysts and their matrix in many silicic volcanic rocks (e.g. Noble and

Editorial responsibility: MA Clynne

C. Deniel (✉)
Laboratoire Magmas et Volcans, UMR 6524 CNRS, OPGC, UBP,
5 rue Kessler,
63038 Clermont-Ferrand cedex, France
e-mail: C.Deniel@opgc.univ-bpclermont.fr

Hedge 1969; Stuckless and O'Neil 1973; Futa et al. 1981; Duffield and Ruiz 1992; Christensen and DePaolo 1993; Wolff et al. 1999). Over the last decade, both in situ measurements and/or analyses on much smaller samples have become available (e.g. Christensen et al. 1995; Davidson and Tepley 1997; Charlier et al. 2006) allowing Sr isotopic heterogeneities at the mineral and sub-mineral scale to be documented. Such studies were often performed on highly evolved compositions, mainly on feldspars but also on biotite (e.g. Davidson and Tepley 1997; Knesel et al. 1999; Tepley et al. 2000; Charlier et al. 2006). These heterogeneities are usually associated with petrological and compositional variations suggesting that these crystals had complex crystallization histories and may originate from distinct magmas and/or have been affected by significant contamination/inheritance processes. Feldspar has often been studied in highly evolved lavas as it is usually a main phenocryst phase and also the main repository for Sr (e.g. plagioclase in Cerro Toledo rhyolites, Stix and Gorton 1990; sanidine in the Bishop Tuff, Halliday et al. 1984) in these rocks. As these lavas, especially the peralkaline ones, are often characterized by high Rb/Sr ratios, due to their generally very low Sr contents, this has important implications on the meaning of Sr isotopes in such rocks.

In-situ isotope profiles across phenocrysts obviously record petrogenetic processes that are masked in whole-rock Sr isotope studies. They highlight the limitations inherent to whole-rock analyses of phenocryst-rich volcanic rocks. Seeing the complexity of the isotopic Sr patterns in feldspars and other mineral phenocrysts and their groundmass, the significance of Sr isotopes on whole-rocks is really questionable (e.g. Davidson et al. 2005). Multiple open system processes clearly operate in a given magmatic system but unravelling their complexity by whole-rock data alone is generally impossible.

In this paper, the variation of whole-rock Sr isotopes and Rb–Sr contents in highly evolved low-Sr samples (pantelleritic rhyolites) from the Main Ethiopian Rift (MER) is investigated. Significant heterogeneities are observed in various types of samples (pumices, obsidian and lava) and their meaning is discussed. Even mostly aphyric samples are concerned by such heterogeneities, suggesting that they exist at a small-scale and are not necessarily related to contaminated/inherited crystals. Whole-rock Sr isotope data are not only averages of a potentially heterogeneous material, but they may lack of accuracy in highly evolved rocks, even fresh and apparently homogeneous, depending on the scale of sampling. Thus, unreplicated measurements should always be used with great caution in the petrogenetic modeling of such rocks. However, multiple whole-rock Sr isotope determinations, combined with other geochemical and isotopic data, may give useful constraints on the shallow level evolution of these magmas, especially on crustal contamination and/or fluid interaction processes.

Background

Geological setting

The Main Ethiopian Rift and Afar represent the northernmost part of the East African Rift. This tectonic structure is a famous example of a young intracontinental rift. It is part of the Afro-Arabian rift system to which a large continental flood basalt province is associated (e.g. Mohr and Zanettin 1988). The Ethiopian volcanic province is dominated by up to 300,000 km^3 of mid-Tertiary basaltic lavas associated with felsic products. In the Ethiopian rift valley, the proportion of felsic volcanic products is about 90% of the total volume of erupted material (Mohr 1992). In the studied MER sector, most of the huge volumes of felsic alkaline rocks either have a fissural origin or are related to large volcano-tectonic collapses (Boccaletti et al. 1995).

The studied samples belong to three different ignimbritic units from the Asela–Ziway area, about 125 km south-east of Addis Ababa, on the eastern shoulder of the MER. These volcanic rocks are younger than 1.7 Ma (WoldeGabriel et al. 1990) and are related to the most recent tectonic phases of the MER formation (Abebe et al. 1997). The precise location of these samples as well as the detailed stratigraphy of the corresponding volcanological units are available in Trua et al. (1999). The oldest units (Asela and Tulu Moye-Hate, 1.7–0.83 Ma) represent the unimodal felsic magmatism overlapping the older bimodal Chilalo volcanism. The youngest unit (Aluto Berecha, 0.83 Ma) belongs to a bimodal magmatic suite (Trua et al. 1999) erupted between 0.83 Ma and 0.02 Ma (WoldeGabriel et al. 1990).

Samples

The analyzed samples are peralkaline rhyolites (obsidian, lava, pumices) belonging to pantelleritic ignimbrites and minor lava domes and flows studied by Trua et al. (1999) and Deniel et al. (2000). The main characteristics of the analyzed samples are summarized in Table 1. The mineral analyses were published elsewhere (Trua et al. 1999). Note that the composition of the various minerals is homogeneous within a single sample and that the range of anorthoclase and pyroxene compositions among the samples is very limited.

The Asela and Tulu Moye-Hate samples (lava domes and pumice flows) are mainly vitrophyric with scarce small crystals of quartz and anorthoclase ($Or_{31–28}$) with fairly homogeneous compositions (LA7 and LA13). Sodium-rich augite ($Wo_{41}En_2$) and sporadic small crystals of aenigmatite

Table 1 Main petrological and chemical features of the Asela–Ziway highly evolved rocks

Volcanological unit	Samples	Main characteristics	LOI (wt.%)	SiO_2 (wt.%)
Asela	LA7	Grey pumice in ignimbrite vitrophyric with scarce anorthoclase (Or_{31}) crystals (<0.5 mm size)	3.54	70.48
Tulu Moye-Hate	LA13	Large dark glassy fiamme in ignimbrite 2–3 vol.% of heterogeneously distributed anorthoclase (Or_{28}) crystals (<0.5–3 mm size) or crystal clusters	0.72	70.80
	LA16	Very homogeneous aphyric dark obsidian (lava dome)	0.55	71.70
Aluto Berecha	AS12	Grey lava, aphyric, non vesiculated (lava dome) heterogeneous microcrystalline texture with alkali feldspar microcrystals and inhomogeneously distributed pyroxene/amphibole microcrystals	0.53	74.82
	LA46	Beige aphyric pumice	4.52	68.57
	LA38	Porphyritic obsidian (lava dome) about 15 vol.% anorthoclase ($Or_{37–36}$) crystals (<1–3 mm size), subordinate (2 vol.%) Na-rich augite ($Wo_{41–40}En_{2–1}$) phenocrysts, aenigmatite microphenocrysts ± fayalite ± quartz (<<1 vol.%)	0.68	71.05

were also encountered in some other samples belonging to these volcanological units (Trua et al. 1999). The ignimbrites locally contain large dark glassy fiammes with abundant anorthoclase phenocrysts (LA13) or sanidine (Trua et al. 1999).

The Aluto Berecha felsic rocks mainly consist of porphyritic pantellerites with anorthoclase ($Or_{37–36}$) and subordinate sodium-rich augite ($Wo_{41–40}En_{2–1}$) phenocrysts, aenigmatite microphenocrysts ± fayalite ± quartz (LA38). The groundmass texture of the lavas from the domes may be heterogeneous, with alkali feldspar microcrystals (AS12).

All the samples were fresh and devoid of xenoliths, both in hand specimen and in thin sections. The loss on ignition (LOI) is 0.53 to 0.72 wt.% for the lava and the obsidian. It is 3.5 and 4.5 wt.% in the pumices. Such high LOI are common for pumices because of the high volatile content of the corresponding magmas associated to explosive eruptions. However, the progressive hydration of their glass components with time may also partly account for these high LOI (e.g. Schmitz and Smith 2004).

A two-stage model for the genesis of these highly evolved rhyolites

The petrogenesis of the Asela–Ziway rhyolites was already discussed on the basis of petrological, geochemical and isotopic (Nd, Pb) data (Trua et al. 1999; Deniel et al. 2000). A two-stage model involving small degrees (10%) of equilibrium partial melting of a mafic lower crust (underplated magmas?), followed by moderate degrees (40%) of crystal fractionation (mostly Na-feldspar) may account for the geochemical characteristics of the least differentiated rhyolite (LA38). The predominance of alkali feldspar fractionation over that of plagioclase is also supported by the mineral assemblage of LA38. Its Nd and Pb isotope compositions, almost identical to those of the local basalt used for these calculations, are also compatible with such a model. The negative Ba, Sr, P, Eu and Ti anomalies of all these rhyolites also suggest low-pressure crystal fractionation of alkali feldspar, plagioclase, titanomagnetite and apatite in their genesis, as also suggested by their phenocryst assemblages. It is also compatible with the model of Caricchi et al. (2006) requiring polybaric differentiation starting at elevated pressures for the genesis of other peralkaline magmas from the MER. According to these authors, extensive crustal thinning and intense fracturing of the crust would allow the rapid ascent of parental magmas from the lower crust into shallow magma reservoirs where differentiation/fractionation under low pressure conditions would occur. This two-stage model, with varying degrees of partial melting (5–10%) and crystal fractionation (20–40%), may account for the geochemical and Nd, Pb isotope characteristics of the Asela–Ziway peralkaline rhyolites. AS12, the most evolved sample clearly requires a much higher degree of crystal fractionation. However, its Nd and Pb isotope compositions are within the range observed in the associated basalts and thus do not give evidence for significant upper crustal contamination.

More recently, the effects of repetitive emplacement of basaltic intrusions over 10^5–10^6 years on thermal evolution and melt generation in the crust have been studied (e.g. Petford and Gallagher 2001; Annen and Sparks 2002). The initial incubation period, with basaltic intrusions solidification, would be consistent with the development of an underplated mafic crust (Annen and Sparks 2002). Furthermore, such deep crustal intrusions causing long-lived thermal anomalies would be prone to remelting processes during

subsequent magmatic episodes (Petford and Gallagher 2001; Annen and Sparks 2002). Melt generation would thus involve simultaneous cooling and crystallization of the intruding basalts and partial melting of both the new basaltic crust and the pre-existing old crust (e.g. Annen and Sparks 2002), the melting proportions of these components being controlled by the temperature and water content of the intruded basalts and the fertility of the country rocks. In the MER sector, both the asthenospheric upwelling (Mahatsente et al. 1999) and the protracted magmatic activity would have favoured the persistence of such a thermal anomaly. It is consistent with the regional scarcity of basalts and intermediate products associated with the MER peralkaline rhyolites and would be compatible with the involvement of lower crustal contamination during the differentiation of the Asela–Ziway basic to intermediate rocks (Trua et al. 1999).

Methods

Samples (0.5 to 0.8 kg) selected for isotope composition and isotope dilution analyses (Trua et al. 1999, this work) were chipped to less than 8 mm fragments in a steel jaw crusher. Each crushed and homogenized sample was then split into a main aliquot (saved) and a small one (used for isotope analyses). After screening through sieves, this small aliquot represented 15 g (pumices) and 30 g (lavas) of chips (2–8 mm in size). From this homogenized aliquot, individual batches (1 to 3 g each) of rock chips (2–4 mm) were then handpicked to ensure freshness before further processing in the laboratory, either directly as chips or after crushing to powders (see below).

Sr isotope composition (IC) analyses

Some rock chips (about 0.8–1 g) were leached in 6 M HCl at 100°C, for 45 min and rinsed twice with water. These samples were then digested and processed in the laboratory for Pb, Nd and Sr isotope composition measurements by thermal ionisation mass spectrometry (TIMS) as described in Deniel et al. (1994). Pb and Nd isotope results were published in Trua et al. (1999) with data on basaltic rocks from the same area. Analyses performed on chipped rock samples are indicated in Table 2 with the prefix C.

Some rock chips (2–3 g) were leached with 6 M HCl at 100°C for 45 min and rinsed twice with water. They were dried and crushed to powders in an agate mortar and 0.3 g used for Sr isotope analyses. Samples processed in this way are indicated by the prefix P in Table 2.

Hydrochloric acid distilled in sub-boiling silica glass still (Quartex, Paris) and water purified through a Milli-Q system (Millipore) were used throughout.

Sr isotope dilution (ID) analyses

The very low Sr (2–15 μg/g) and high Rb (98–240 μg/g) contents of highly evolved rocks result in high Rb/Sr ratios which induce significant uncertainties on initial Sr isotope compositions, even for young rocks (<0.5–1 Ma). Consequently, it is critical to measure both Sr and Rb contents as accurately as possible on the same sample fraction used for $^{87}Sr/^{86}Sr$ analysis. Thus, many analyses of these Ethiopian rocks were performed by isotope dilution (ID) and TIMS.

For these analyses, powders were prepared as described for the Sr isotope composition measurements. For each Sr ID analysis a mixed ^{85}Rb–^{84}Sr spike was added to 0.3 g of powder before digestion with mixed HF–HNO_3–$HClO_4$ acids. After drying, samples were taken up in 6 M HCl, warmed, and evaporated before final dissolution in 2.5 M HCl for separation of Rb and Sr on a cationic resin. Perfect isolation of Sr from Rb is necessary for accurate determinations of $^{87}Sr/^{86}Sr$ ratios because of the isobaric interference at $m/z=87$ and the highly effective ionization of Rb by TIMS. To ensure high quality TIMS measurements of these Sr-depleted samples, Sr was thus purified from Rb using the Sr.Spec. extraction chromatographic material (Pin et al. 1994). Rb was further purified from matrix elements using zirconium phosphate as a cation exchanger (Pankhurst and O'Nions 1973; Pin et al. 2003). To overcome the potentially significant memory effects of the Sr.Spec. extraction chromatographic material (Pin and Bassin 1992; Pin et al. 1994), 6 M hydrochloric acid was used to clean the columns (Deniel and Pin 2001). After washing the 250 μl of Sr.Spec. with 5 ml of 6 M HCl, the resettling was performed in about 5 ml of 0.05 M HNO_3 before further washing with 5 ml of 0.05 M HNO_3.

Mass spectrometry

Rb was loaded onto Ta filaments and measured on a Cameca TSN 206SA single collector mass spectrometer. Sr was loaded onto tungsten filaments covered with a tantalum gel as an ion emitter (Birck 1986). All the Sr isotope measurements were performed on a VG 54E mass spectrometer in the dynamic double collection mode. $^{87}Sr/^{86}Sr$ ratios are normalized to $^{86}Sr/^{88}Sr=0.1194$ and given relative to a $^{87}Sr/^{86}Sr=0.710219\pm45$ (2 SD, 22 measurements) for the NBS SRM 987 standard. The internal errors (2 SE) of Sr isotope measurements are given in Table 2 and range mostly between 2×10^{-5} and 5×10^{-5}. A 2% error is associated to the determination of $^{87}Rb/^{86}Sr$ ratios by ID-TIMS. The maximum total Sr blank (1 ng) was negligible relative to the amount of Sr analyzed.

Results

Both measured ($^{87}Sr/^{86}Sr_m$) and initial ($^{87}Sr/^{86}Sr_{in}$) Sr isotope ratios and the Rb and Sr contents are reported in Table 2. The ages used to calculate the $^{87}Sr/^{86}Sr_{in}$ are those published for the corresponding volcanological units (WoldeGabriel et al. 1990). These $^{87}Sr/^{86}Sr_{in}$ were calculated in two different ways. For isotope composition analyses (IC), the XRF or ICP-MS Rb and Sr contents (Trua et al. 1999) were used. For isotope dilution analyses (ID), the Rb and Sr contents determined on the same sample aliquot as the Sr isotope ratio were used.

Despite variation among the data, some AS12 results define a positive correlation between $^{87}Sr/^{86}Sr_m$ and $^{87}Rb/^{86}Sr$, giving an apparent isochron age at 0.7 Ma (Table 2). This age and the mean square of weighted deviates (MSWD) reported were calculated with ISOPLOT, Model 1 (Ludwig, http://www.bgc.org/klprogrammenu.html).

Rb and Sr contents

Rb and Sr contents were measured by both XRF and ICP-MS, with expected uncertainties of 5–10% for Rb (>100 μg/g) and up to 25% or even more for Sr (1 to 15 μg/g). Despite a very high consistency between Sr contents measured by XRF and ICP-MS in four out of six samples, a significant variation is observed for both Sr and Rb in some samples. It is 11% and 19–21% for Sr and Rb, respectively, for LA7 and LA46. A 11–12% difference between XRF and ICP-MS is still observed for Rb in LA16 and AS12. The Rb content measured by ICP-MS is systematically lower than that measured by XRF, except for LA38 (almost identical). The resulting difference of the $^{87}Rb/^{86}Sr$ ratio between the two data sets is 7–12%, except for LA38 (2%).

The accuracy of the XRF and ICP-MS data (especially for Sr) can only be evaluated by comparison with the ID-TIMS data which are the most precise of any. Most ID Rb contents range between the XRF and ICP-MS values (Table 2). However, a higher discrepancy is observed for LA38 (5%) and especially AS12 (16%) for which one ID measurement is clearly outside this range. The consistency between ID and XRF/ICP-MS Sr values is relatively poor, except for LA13 (15%) and LA16 (3%). For LA7, the range of variation among ID data is much larger than the difference between XRF and ICP-MS values whereas for LA46, the ID Sr content is about four times lower than the XRF/ICP-MS values. For the other samples, ID Sr is systematically lower than both XRF and ICP-MS Sr by 30% to 50%. Such discrepancies between XRF/ICP-MS and isotope dilution Sr data are not surprising and confirm the poor accuracy of XRF and ICP-MS measurements for such low Sr concentrations. Only isotope dilution combined with TIMS or ICP-MS can give precise and accurate Sr determinations at such a low level of concentration.

Furthermore, the variation of Rb and/or Sr contents measured by isotope dilution is large within a single sample (except for obsidian LA16 and LA38), ranging between 9% and 28% for Rb and between 9% and 121% for Sr. The resulting variation of the $^{87}Rb/^{86}Sr$ ratio is 17–125%, except for LA16 and LA38 (≤3%). This is significantly greater than the analytical uncertainty (2% error) on $^{87}Rb/^{86}Sr$ ratios measured by isotope dilution and suggests the existence of significant Rb and Sr, within sample, heterogeneities.

Sr isotope ratios

Replicate whole-rock $^{87}Sr/^{86}Sr_m$ and $^{87}Sr/^{86}Sr_{in}$ are variable, although to various extents. Samples LA7, LA13 and AS12 are particularly heterogeneous. $^{87}Sr/^{86}Sr_{in}$ variations among replicate isotope dilution (ID) analyses are 660–2,080 ppm (Table 2) for all samples but LA38 and LA16, also homogeneous for their Rb and Sr contents (see previous section). Even larger variations (5,500 and 2,440 ppm) are observed for replicate isotope composition (IC) measurements on both rock chips and powders of LA13 and AS12 (Table 2). For LA7 and LA46, the isotope dilution data cover the whole range of $^{87}Sr/^{86}Sr_{in}$ variation whereas for LA13, the isotope composition data do. Although the range of variation observed with isotope compositions is large for AS12, it is even larger (3,740 ppm) when both isotope dilution and isotope composition data sets are considered. For LA16 and LA38, considering both isotope dilution and isotope composition data increases the range of variation to 180 and 205 ppm, respectively.

The effect of using the XRF or ICP-MS Rb and Sr data for the calculation of the $^{87}Sr/^{86}Sr_{in}$ is also illustrated in Table 2. When only one IC measurement was performed (LA7, LA16, LA46 and LA38), the initial Sr isotope ratios were calculated with the two data sets. The difference between both results is within the 2 SE of the Sr isotope measurements themselves. It must be noted that for these four samples, the $^{87}Rb/^{86}Sr$ ratios are relatively low (9–52). When various IC measurements were performed (LA13 and AS12), the incidence of using the XRF or ICP-MS data was illustrated on one measurement. For these samples with higher $^{87}Rb/^{86}Sr$ (125–184), the difference on the initial Sr isotope ratios is larger than the 2 SE of the isotope measurements.

The total range of $^{87}Sr/^{86}Sr$ variation due to in situ radioactive decay of ^{87}Rb is 300 to 3,300 ppm (Table 2). This enrichment is important not only because of the relatively old ages (reaching 1.7 Ma for LA7) but also, mainly, because of the high $^{87}Rb/^{86}Sr$ ratios, as for AS12 and LA13. Figure 1 illustrates, with the ID data, that an accurate age of the lavas

Table 2 Whole-rock Sr isotope data for highly evolved lavas from Asela–Ziway (MER, Ethiopia)

Samples	Analyses	$^{87}Sr/^{86}Sr_m$	2SE ($\times10^{-5}$)	Rb (μg/g)	Sr (μg/g)	$^{87}Rb/^{86}Sr$	$(^{87}Sr/^{86}Sr)_{in}$ (a)	$(^{87}Sr/^{86}Sr)_{in}$ (b)	Sr_{in} variation	Sr_m–(Sr_{in} (a))
LA7										
Asela (1.7 Ma)	P1a (*ID*)	0.70496	4	134.7	14.8	26.4	0.70432		2,080 ppm	0.00064
	P2a (*ID*)	0.70465	3	137.2	6.7	59.4	0.70322		(on ID results)	0.00143
	P3a (*ID*)	0.70508	4	143.1	7.6	54.6	0.70376			0.00132
	P3b (*ID*)	0.70505	4	144.3	7.6	55.1	0.70372			0.00133
	P4a (*ID*)	0.70618	9	134.1	8.6	45.2	0.70509			0.00109
	P4b (*ID*)	0.70646	4	138.2	8.3	48.3	0.70529			0.00117
	P2b (*IC*)	0.70464	4	151[c]	10[c]	43.8	0.70358		70 ppm	0.00106
				127[d]	9[d]	40.9	0.70365		(on IC results)	0.00099
LA13										
Tulu Moye-Hate (0.83–1.7 Ma)	P1a (*ID*)	0.70929	4	126.1	2.2	166	0.70733	0.70528	730 ppm	0.00196
	P1b (*ID*)	0.70936	3	123.4	2.1	170	0.70735	0.70525	(on ID results)	0.00201
	P2a (*ID*)	0.70860	4	124	2.3	156	0.70675	0.70482		0.00184
	P2b (*ID*)	0.70834	6	115.6	2.3	146	0.70662	0.70482		0.00172
	P1c (*IC*)	0.70933	2	127[c]	2[c]	184	0.70716	0.70488	5,500 ppm	0.00217
	P3a (*IC*)	0.70818	4	127[c]	2[c]	184	0.70601	0.70373	(on IC results)	0.00217
	P3b (*IC*)	0.70825	4	127[c]	2[c]	184	0.70608	0.70380		0.00217
	C4 (*IC*)	0.71365	3	127[c]	2[c]	184	0.71148	0.70921		0.00217
				113[d]	2[d]	164	0.71172	0.70970		0.00193
	C5 (*IC*)	0.71368	2	127[c]	2[c]	184	0.71151	0.70923		0.00217
LA16										
Tulu Moye-Hate (0.83–1.7 Ma)	P1a (*ID*)	0.70558	3	118.5	6.8	50.5	0.70499	0.70436	7 ppm (on ID results)	0.00060
	P1b (*ID*)	0.70559	4	120.6	6.9	50.7	0.70499	0.70437	180 ppm (on ID + IC)	0.00060
	C2 (*IC*)	0.70542	3	125[c]	7[c]	51.8	0.70481	0.70417	130 ppm (on IC results)	0.00061
				112[d]	7[d]	46.4	0.70488	0.70430		0.00055
AS12										
Aluto Berecha (0.83 Ma)	P1a (*ID*)	0.70886	4	232.6	2.9	233	0.70612		990 ppm	0.00274
	P2a (*ID*)	0.70845	5	218.2	3.5	181	0.70632		(on ID results)	0.00213
	P3 (*ID*)	0.70851	4	279.8	3.2	254	0.70552			0.00299
Pseudoisochron age	**P4a (*ID*)**	0.70875	5	233.1	2.4	282	0.70543		3,740 ppm	0.00332
0.70±0.18 Ma	P4b (*ID*)	0.70850	5	227.2	2.45	269	0.70533		(on ID + IC results)	0.00317
MSWD=1.02	**P4c (*ID*)**	0.70875	5	224.9	2.36	276	0.70549			0.00326
	P4d (*ID*)	0.70873	4	224.6	2.36	276	0.70547			0.00325
	P1b (*IC*)	0.70889	3	240[c]	5[c]	139	0.70725		2,440 ppm	0.00164
	P2b (*IC*)	0.70828	10	240[c]	5[c]	139	0.70664		(on IC results)	0.00164
	C5 (*IC*)	0.70902	2	240[c]	5[c]	139	0.70738			0.00164
				216[d]	5[d]	125	0.70754			0.00148
	C6 (*IC*)	0.71072	2	240[c]	5[c]	139	0.70908			0.00164
	C7 (*IC*)	0.70977	4	240[c]	5[c]	139	0.70813			0.00164
	C8 (*IC*)	0.70954	4	240[c]	5[c]	139	0.70790			0.00164

LA46										
Aluto Berecha (0.83 Ma)	P1a (*ID*)	0.70675	9	117.3	13.7	24.8	0.70646	660 ppm		0.00029
	P1b (*ID*)	0.70609	2	127.6	14.7	25.2	0.70580	(on ID results)		0.00030
	P2a (*ID*)	0.70632	4	118.1	10.8	31.7	0.70595			0.00037
	P2b (*ID*)	0.70627	5	118.1	10.7	32.0	0.70589			0.00038
	P2c (*ID*)	0.70640	3	119	10.7	32.3	0.70602			0.00038
	C3 (*IC*)	0.70629		130[c]	40[c]	9.4	0.70617	9 ppm		0.00011
				107[d]	36[d]	8.6	0.70618	(on IC results)		0.00010
LA38										
Aluto Berecha (0.83 Ma)	P1a (*ID*)	0.70471	4	98.2	4	71.2	0.70387	45 ppm (on ID results)		0.00084
	P1b (*ID*)	0.70478	3	106.1	4.2	73.3	0.70392	205 ppm (on ID + IC)		0.00086
	C2 (*IC*)	0.70427	2	99[c]	6[c]	47.9	0.70371	11 ppm (on IC results)		0.00056
				101[d]	6[d]	48.8	0.70370			0.00057

Both measured ($^{87}Sr/^{86}Sr_m$ or Sr_m) and initial ($^{87}Sr/^{86}Sr_{in}$ or Sr_{in}, calculated at the age of the sample) Sr isotope ratios are given. Analyses were performed, either directly on rock chips (C) leached just before chemistry, or on powders (P) prepared from leached rock chips. For each analysis, the number indicates the batch of rock chips and the letter a separate measurement of that batch. For the two Tulu Moye-Hate samples, $^{87}Sr/^{86}Sr_{in}$ ratios are given for 0.83 Ma (a) and 1.7 Ma (b). The analyses used for the pseudoisochron calculations are in bold character. Rb and Sr contents were determined by ID-TIMS except [c] and [d] by XRF and ICP-MS, respectively

ID isotope dilution, *IC* isotope composition

is absolutely required to make the appropriate age correction and get the proper initial $^{87}Sr/^{86}Sr$ ratios. Indeed, for LA16, and especially LA13, it is obvious that the uncertainty on the age of the Tulu Moye-Hate unit has a drastic effect on the intial Sr ratio that is calculated. Note also that for these samples, the range of $^{87}Sr/^{86}Sr_{in}$ variation for ID measurements is higher at 0.8 Ma than at 1.7 Ma (700 and 400 ppm, respectively, for LA13) as outlined by other authors (e.g. Vidal et al. 1984).

Discussion

True initial Sr isotope heterogeneity

The observed Sr isotope variations could be related to analytical problems. However, these rocks were fresh and analyzed at the same time as the less differentiated lavas from the same area. A good reproducibility of the Sr isotopic compositions (including isotope dilution measurements) was systematically observed for basic to intermediate rocks (Trua et al. 1999). The poor reproducibility observed among the highly evolved samples concerns both isotope dilution and isotope composition measurements. Problems related to incomplete equilibration between spike and sample would have only affected the isotope dilution measurements. Furthermore, such problems would not have been systematically restricted to the highly evolved samples. Contamination during processing of these Sr depleted samples, and especially during separation of Sr, seems precluded given the total blanks measured during the period of analyses. Furthermore, it would not account for the significant variation of Rb content observed among replicate measurements (28% for ID analyses in AS12). Rhyolites (pumice and obsidian, 6 Ma and 0.15–0.12 Ma, 131 and 89 μg/g Sr, respectively) from Turkey were also analyzed using the same analytical procedures and gave reproducible Sr isotope data (Deniel et al. 1998). Although these two samples were duplicated only once, it was after two distinct leaching procedures on two different aliquots of rock chips which could have been a factor of additional variation.

Note also that replicate Pb and Nd isotopic compositions measured at the same time on the Asela–Ziway, basic to highly evolved samples, were consistently reproducible (Trua et al. 1999). It is thus probable that the $^{87}Sr/^{86}Sr_{in}$ variations observed in MER samples reflect true isotopic heterogeneities of the analyzed pantelleritic samples. Many studies on highly evolved rocks from various volcanic systems have documented Sr isotope heterogeneity of the related volcanic units (e.g. Halliday et al. 1984, 1989; Davies and MacDonald 1987; Hildreth et al. 1991; Duffield and Ruiz 1992; McCulloch et al. 1994; Bohrson and Reid 1997; Snyder et al. 2004). However, at the sample scale, it

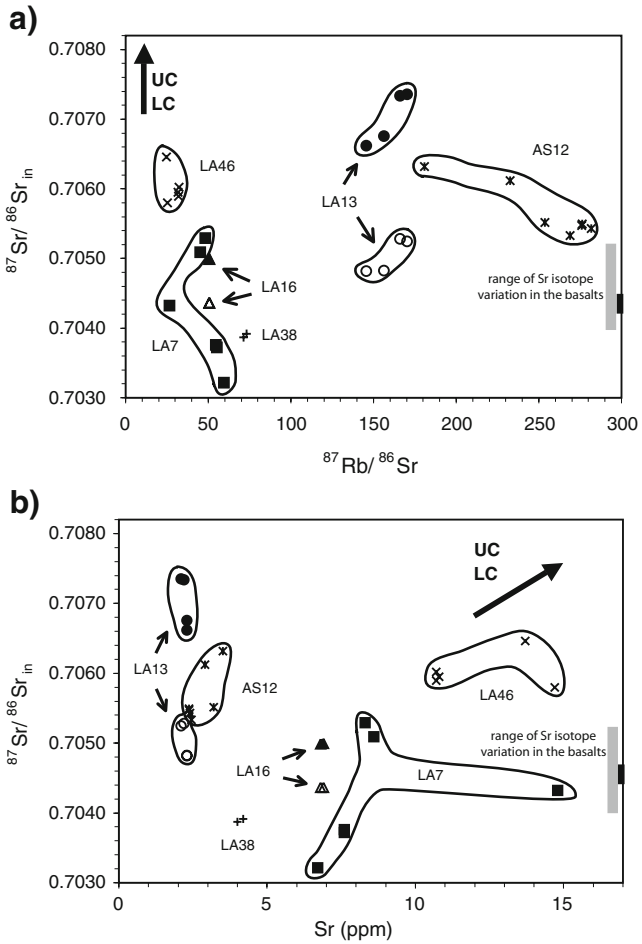

Fig. 1 $^{87}Sr/^{86}Sr_{in}$ of Asela–Ziway highly evolved rocks versus **a** $^{87}Rb/^{86}Sr$ and **b** Sr concentration. For the two Tulu Moye-Hate samples, initial ratios calculated for 1.7 and 0.83 Ma (maximum and minimum ages reported in Trua et al. 1999) are represented by *open* and *close* symbols, respectively. Note that only the isotope dilution (ID in Table 2) data are plotted. *Arrows* point towards upper (UC) and lower (LC) crustal compositions. *Black* and *grey lines* along the *y* axis illlustrate the range of Sr isotope variation (Trua et al. 1999) observed in associated old (Chilalo and Eastern Margin, 2.3–1.3 Ma) and young (Galo Salen, 0.29 Ma) basalts (WoldeGabriel et al. 1990), respectively

has usually been documented through the variation observed between the $^{87}Sr/^{86}Sr_{in}$ of the glass and various minerals (see references in "Introduction").

Isotope composition versus isotope dilution data

For LA7 and LA13, the variation observed among ID $^{87}Sr/^{86}Sr_{in}$ on powders from distinct aliquots of rock chips is significantly outside the errors on both $^{87}Sr/^{86}Sr_m$ and ID $^{87}Rb/^{86}Sr$. However, for AS12, the four aliquots define two groups of values and for LA46, there is some overlap despite significant variation of the ID $^{87}Rb/^{86}Sr$.

Irrespective of this variation among replicate ID data, the Sr_{in} obtained between replicate analyses of a single aliquot of rock chips are generally consistent within the 2 SE of $^{87}Sr/^{86}Sr_m$. This is still true for LA13 (P2a, P2b) if the 2% error on $^{87}Rb/^{86}Sr$ is taken into account. However, for LA7 (P4a with a higher 2 SE, P4b) and LA46 (P1a, P1b), the larger variations observed are outside the analytical uncertainty, at variance with what is observed for some other replicate ID data sets on the same samples (P3a, P3b and P2a, P2b, P2c, respectively) (Table 2).

Furthermore, the variations among isotope composition data are higher than those observed among isotope dilution data (LA13, AS12 in Table 2). When IC and ID data are available on powders prepared from the same aliquot of rock chips, the $^{87}Sr/^{86}Sr_m$ are consistent within analytical error, except for AS12 (P2a, P2b). However, the 2 SE of the $^{87}Sr/^{86}Sr_m$ of P2b is much higher than for most measurements. Note that for this sample, P1a (ID) and P1b (IC) are consistent.

The isotope compositions measured on rock chips are generally significantly different from ID and IC measurements on powders, LA13 being an extreme case. A large variation among distinct aliquots of rock chips is also observed for AS12.

Although all these data consistently suggest a high Sr isotope heterogeneity of the samples, they cannot be strictly compared. For IC data, calculations of $^{87}Sr/^{86}Sr_{in}$ with XRF and/or ICP-MS data do not take into account the possible concomitant variation of the $^{87}Rb/^{86}Sr$, either due to intrinsic heterogeneity of the samples or related to leaching before chemistry, that may introduce a bias on the $^{87}Sr/^{86}Sr_{in}$. For this reason, the diagrams in Figs. 1 and 2 and the related discussion are based on ID measurements only. Furthermore, a bias between analyses of rock chips (C analyses) and powders (P analyses), prepared from a larger amount of rock chips (see "Methods" section), may also exist because of the corresponding distinct sampling scales. The smaller scale of sampling for rock chips may potentially introduce a bias towards distinct signature and/or higher heterogeneity, as observed for LA13 and AS12.

Sr isotope heterogeneity versus petrology and sample size

Only in some of the analyzed samples are $^{87}Sr/^{86}Sr_{in}$ variations associated with significant petrological features that may account for these heterogeneities. Among the Asela and Tulu Moye-Hate samples, only the LA16 obsidian, very fresh, homogeneous and aphyric, gives reproducible Sr isotope results. The LA7 pumice is highly heterogeneous in $^{87}Sr/^{86}Sr_{in}$ despite the apparent compositional homogeneity of its scarce feldspar phenocrysts (Trua et al. 1999). LA13 displays even more variation in $^{87}Sr/^{86}Sr_{in}$. Feldspar crystals distributed as clusters in this otherwise homogeneous glassy fiamme could account for this heterogeneity. The possible sampling of such feldspar clusters

in rock chips (C, Table 2) might account for their distinct isotopic signatures. Indeed, the presence of inherited crystals recording distinct isotopic signatures has been reported for highly evolved rocks from various volcanic systems (e.g. Noble and Hedge 1969; Christensen and DePaolo 1993; Tepley et al. 1999; Wolff et al. 1999; Snyder et al. 2004; Charlier et al. 2006). In other cases, the contrast between phenocrysts and glass has been interpreted as the result of progressive Sr contamination or post-eruptive surface alteration (e.g. Halliday et al. 1984; Duffield and Ruiz 1998; Knesel et al. 1999; Snyder et al. 2004).

The LA38 Aluto Berecha sample is homogeneous regarding both its $^{87}Sr/^{86}Sr_{in}$ and feldspar and clinopyroxene compositions (Trua et al. 1999 and Table 1). The LA46 pumice and AS12 lava are heterogeneous in both $^{87}Sr/^{86}Sr_{in}$ and Rb–Sr contents (as measured by ID). Although no obvious petrological heterogeneity is observed in AS12, it displays a significant textural heterogeneity (grain size and nature of the microcrystals). This could reflect the occurrence of magmas with slightly different compositions, volatile contents and viscosities as expected in lava domes. Furthermore, negative and positive trends are observed among AS12 ID data (Fig. 1a, b), suggesting that the isotopic variations in this lava are mainly related to its Sr contents. No such correlation is observed with Rb despite 28% variation. Such trends would be compatible with the mixing of a magmatic component characterized by a low Sr content and $^{87}Sr/^{86}Sr$ and another component with higher Sr content and more radiogenic $^{87}Sr/^{86}Sr$. It could be a crustal component that would also account for the strong variation of Rb contents. AS12 is the most evolved rhyolite with extreme fractionation suggesting a higher residence time at upper crustal levels compared with the other samples. Alternatively, the involvement of fluids could be consistent with AS12 textural characteristics and Sr isotope pattern as discussed hereafter, provided these fluids were enriched in ^{87}Sr. The apparent isochron age defined by the four analyses corresponding to the lowest $^{87}Sr/^{86}Sr_{in}$ is consistent with the published age of the Aluto Berecha unit (WoldeGabriel et al. 1990) and could correspond to fluid unmodified domains. However, more data would be required to better constrain such hypothesis.

Only pumices exhibit relatively high LOI (Table 1), although not exceptional for these kinds of samples. Gain of Sr has been described both on crystallization and hydration of glassy peralkaline silicic rocks (Noble 1967; Baker and Henage 1977; Weaver et al. 1990) whereas the behaviour of Rb during circulation of groundwater is not so well established (e.g. Noble 1967; Weaver et al. 1990). These secondary processes may account for the $^{87}Sr/^{86}Sr_{in}$ heterogeneity in pumices. Although the importance of various secondary processes has been reported for highly evolved volcanic rocks (e.g. Halliday et al. 1984; Snyder et al. 2004), there is no evidence that they may account for the heterogeneities observed in the other, very fresh, MER samples.

The results of this study indicate that (1) Sr heterogeneity (both Rb–Sr contents and $^{87}Sr/^{86}Sr_{in}$) is common in most Sr depleted highly evolved rocks (pumice, aphyric lava, obsidian), not only in samples exhibiting high LOI and/or obvious heterogeneous petrological features and (2) it is hard to predict this degree of isotope heterogeneity and especially its scale.

The preparation of samples performed for this study is similar to that used by many isotope geochemists, especially those involved in Pb isotopes. When Sr and/or Nd isotopes are to be measured, the same material is generally used. It is well known that whole-rock values are only averages and that much petrogenetic information is lost with such data. However, this study suggests that even whole-rock analyses do not necessarily give an accurate average for Sr isotopes in highly evolved rocks, depending on the scale of the heterogeneities (a few millimeters here), the way samples were prepared and their size. In the present case, the samples were homogenized aliquots at each stage but the last step, aliquots of powders from 2–3 g crushed rock chips and especially rock chips themselves (0.8–1 g) (see "Methods" section), apparently sampled small-scale elemental (Rb, Sr) and isotopic heterogeneities. As a result, the average $^{87}Sr/^{86}Sr_{in}$ of the samples cannot be accurately determined. The method good for Pb isotopes is probably not suited for Sr isotopes in such rocks. To get representative Sr isotope averages on such, mostly aphyric, highly evolved peralkaline rocks would require to keep a much larger scale of sampling/homogenization, at least the 15 to 30 g mentioned earlier for these samples (obsidian, lava and pumice). For porphyritic samples, the amount of homogenized material required for analyses would obviously be much larger although it cannot be constrained *a priori* as it will be a characteristic of each sample. Considering the usual approach of isotope geochemists for such analyses, it implies that, in general, no precise mean Sr isotope value is available, through a single whole-rock measurement, for detailed petrogenetic modeling of such rocks.

It is clear that giving the reproducibility of the standard NBS 987 to evaluate the quality of a Sr isotope data set on such samples is inappropiate. The Sr isotope variation observed among multiple analyses of the samples is here two to 120 times the 2 SD (standard deviation) on the NBS 987 mean. Although some replicate analyses with distinct sample digestions may have been performed, they are rarely reported in papers dealing with whole-rock Sr isotope data on highly evolved, Sr depleted samples. The description of the analytical procedures may be given together with the value and reproducibility of the NBS 987 standard (e.g. Heumann and Davies 2002; Heumann et al. 2002; Vasquez and Reid 2002; Snyder et al. 2004) but not systematically. It is also

common to only supply the data concerning the standard (e.g. Karapetian et al. 2001; Gioncada et al. 2003) or, simply, none of this information (e.g. Paquereau Lebti et al. 2006). Furthermore, the Rb and Sr contents used to calculate the $^{87}Sr/^{86}Sr_{in}$ may be XRF or ICP-MS data (e.g. Gioncada et al. 2003; Paquereau Lebti et al. 2006) which result in significant additional errors as discussed above. Sometimes, the age correction is not performed on the data (e.g. Karapetian et al. 2001; Gioncada et al. 2003; Paquereau Lebti et al. 2006) and isotope ratios of different units with variable ages are directly compared to each other and discussed in terms of petrogenesis. More analytical information would be welcome and probably greater caution required when drawing petrogenetic inferences based on such data.

Petrogenetic implications

As multiple whole-rock Sr isotope measurements were performed on these highly evolved volcanic rocks from the MER, it is interesting here to compare the picture given by Nd and Pb isotopes on one hand (Trua et al. 1999) and that given by Sr isotopes on the other hand. The $^{143}Nd/^{144}Nd$ and Pb isotope variations among rhyolites belonging to the older unimodal magmatism (Asela, Tulu Moye-Hate) are within those of the older basalts (Trua et al. 1999 and Fig. 2). The variations among the Aluto Berecha rhyolites belonging to the younger, bimodal magmatism are approximately within those of the associated basaltic rocks. These younger basic rocks are more contaminated by the crust (Late Proterozoic lower crust) than the older basalts. All these data support a genetic link between the basalts and the rhyolites, without obvious crustal contamination of the rhyolites themselves, as modeled by Trua et al. (1999).

The picture given by Sr isotopes in these lavas is clearly much more complicated than that given by Nd and Pb isotopes alone. A large range of $^{87}Sr/^{86}Sr_{in}$ is observed among these MER differentiated samples: 0.70322–0.70735 for individual isotope dilution analyses and 0.70389–0.70701 for their means. The distinction between the two groups of rhyolites is not apparent with Sr isotopes alone (Fig. 2a) although it is clear-cut with either Nd or Pb isotopes (not shown). However, it is apparent in the Pb–Sr and Nd–Sr isotope diagrams (Fig. 2b, c) despite the large Sr isotope heterogeneity of some samples.

For the Aluto Berecha samples, the least radiogenic $^{87}Sr/^{86}Sr_{in}$ is observed in LA38. This ratio is similar to that of the most primitive young basalt, supporting their close genetic link without crustal contamination during shallow level differentiation (Trua et al. 1999). Interestingly, this is one of the rare samples for which $^{87}Sr/^{86}Sr_{in}$ are homogeneous. The two other Aluto Berecha samples, AS12 and LA46, display both heterogeneous and more radiogenic $^{87}Sr/^{86}Sr_{in}$ than LA38. Their Pb and Nd (for LA46) isotope

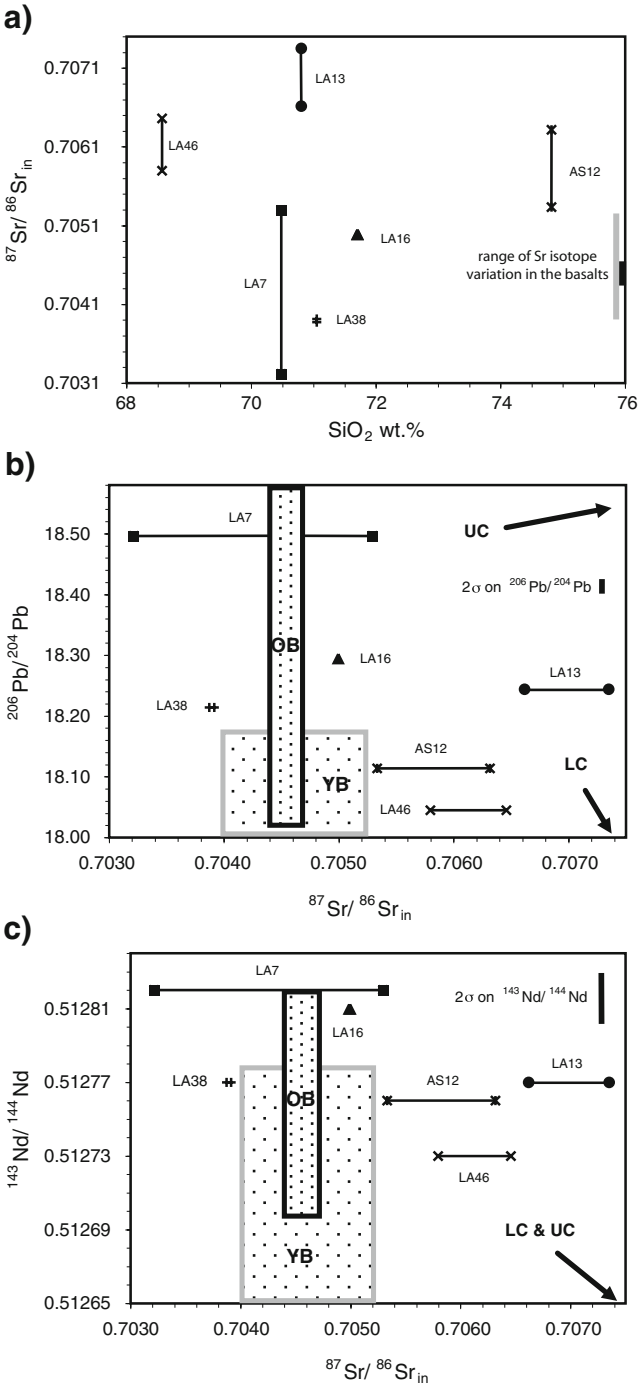

Fig. 2 $^{87}Sr/^{86}Sr_{in}$ of Asela–Ziway highly evolved rocks versus **a** SiO_2 wt.%, **b** $^{206}Pb/^{204}Pb$ and **c** $^{143}Nd/^{144}Nd$. Pb and Nd isotope data are from Trua et al. (1999). Minimum and maximum $^{87}Sr/^{86}Sr_{in}$ ratios for each sample (only ID data) are tied joined by a *black line*. Note their large variation compared to the 2σ error on Pb and Nd isotope ratios. The *black* and *grey lines* (along the *y* axis in **a**) and *rectangles* (in **b** and **c**) indicate the range of isotope variation in the old (OB) and young (YB) basalts, respectively. *Arrows* indicate the trends towards upper and/or lower crust

ratios are also less radiogenic than those of LA38. Their Sr ratios are higher than those of the associated basaltic rocks despite similar Nd and Pb isotope ratios (Fig. 2). These data suggest that a two-stage contamination process may have occurred. The Nd and Pb isotope contrast between the basic magmas and the inferred lower crust (data from Sudan in Davidson and Wilson 1989) is strong. Furthermore, the Nd and Pb contents of these magmas are similar and two to 15 times lower, respectively, than in this crust. Thus, lower crustal contamination of the basic precursors as modeled by Trua et al. (1999) may have significantly modified Nd and Pb isotopes. On the other hand, Sr isotopes would probably be more easily modified in the rhyolites themselves as they are much more depleted in Sr (2–15 μg/g) than the basalts (500 μg/g). Furthermore, the Sr concentration in the upper crust is at least four to 40 times higher than in the rhyolites and the isotopic contrast between both is much larger than between the basaltic precursors and the lower crust. Because of these specific mass balance ratios, the sensitivity of the Sr isotopic system will be much higher at upper crustal levels where the rhyolitic magmas reside during differentiation. The fact that Nd and Pb isotope ratios are slightly less radiogenic in LA46 than in AS12 for similar Sr isotope ratios and despite a seven times higher Sr content in LA46 is consistent with such a two-stage contamination process. Indeed, Sr isotopes suggest that LA46 is more contaminated than AS12 despite a significant lower degree of differentiation. This might indicate that upper crustal contamination is not strictly related to differentiation and occurred at a small-scale in the magmatic system (e.g. Duffield and Ruiz 1992, Duffield et al. 1995). Alternatively, it might reflect the involvement, to various extents, of both crustal contamination and fluid interaction processes.

Although very heterogeneous, the $^{87}Sr/^{86}Sr_{in}$ ratios of the Asela sample overlap the range of Sr ratios observed in the old basalts (Fig. 1, 2) and extend toward both less and more radiogenic values. On the other hand, Nd and Pb isotope ratios are at the more radiogenic end of the old basalt ranges (Fig. 2b, c) suggesting that there was no significant lower crustal contamination. The coexistence of unradiogenic and radiogenic Sr signatures could again be accounted for by shallow level contamination and/or fluid interactions operating on a small-scale, locally preserving the original Sr isotope signature.

The two Tulu-Moye Hate samples display significantly different Sr isotope ratios. LA13 has a significantly more radiogenic Sr signature than LA16, and exhibits only slightly less radiogenic Nd and Pb isotope ratios (Fig. 2). Although both samples display similar SiO_2 content suggesting similar degrees of differentiation, LA13 is significantly more depleted in Sr than LA16 and may have been more sensitive to contamination. $^{143}Nd/^{144}Nd$ in LA16 is similar to the most radiogenic values encountered in the old basalts whereas Pb isotope ratios are in the middle of the range, and $^{87}Sr/^{86}Sr_{in}$ ratios are more radiogenic (Fig. 2). Despite its $^{87}Sr/^{86}Sr_{in}$ homogeneity, LA16 may have been contaminated by the crust too, but to a lower extent than LA13 in which the presence of inherited crystals may also be suspected (see previous section).

Possible contamination processes: upper crustal contamination versus late magmatic fluid interactions

For two samples from Tulu Moye-Hate with the same degree of differentiation, the more Sr-depleted sample is significantly more radiogenic. However, the two Aluto Berecha samples (LA46, AS12), exhibiting distinct degrees of differentiation and Sr contents, display the same $^{87}Sr/^{86}Sr_{in}$. These data suggest that the contamination process is probably not simply related to the degree of differentiation but to the inherent susceptibility of the Sr isotope system in the evolved magma. Furthermore, the coexistence of variously contaminated Sr isotope signatures within individual samples suggests that (1) this contamination process was probably occurring at a small-scale in the magmatic system and (2) the time available before eruption was too short for diffusion to reach isotopic equilibrium.

Random variations of $^{87}Sr/^{86}Sr_{in}$ of bulk-rock samples and concentrates of sanidine phenocrysts on the scale of centimeters to tens of meters have been reported for the Taylor Creek Rhyolite (Reece et al. 1990; Duffield and Ruiz 1992). They were interpreted to reflect dynamic disequilibrium of the assimilation process (<1 wt.% of Proterozoic basement rocks) which was frozen into the rocks by thermal quenching at the time of eruption. Similar small scale heterogeneities observed in the Bishop Tuff (Halliday et al. 1984; Gardner et al. 1991; Lu et al. 1992; Christensen and DePaolo 1993) were reinterpreted in the same way (Duffield et al. 1995). According to Duffield and Ruiz (1998), the isotopic disequilibrium between feldspar phenocrysts and their groundmass in the Taylor Creek Rhyolite would be accounted for by incremental contamination of the magma as wall-rocks melt incongruently. Such a model of selective contamination, probably occurring in a thin layer at the periphery of the magmatic reservoir (Duffield and Ruiz 1992, Duffield et al. 1995), could account for some $^{87}Sr/^{86}Sr_{in}$ heterogeneity in the MER rhyolites.

However, the involvement of ^{87}Sr-rich fluids could provide an alternative mechanism for generating the small-scale scatter of $^{87}Sr/^{86}Sr$. This process, more pervasive than selective crustal contamination, would probably better account for the strong isotopic heterogeneities observed in some samples, and especially in AS12. High Cl and F contents have been found in glass and apatite of MER evolved lavas (Trua et al. 1999). High F contents of natural waters of the MER have been related to water

having percolated through felsic and alkaline volcanic rocks from this area (Chernet et al. 1997). These data suggest that halogen-rich fluids were associated with these lavas, especially in their late stage evolution. AS12, the most evolved sample exhibits an extreme enrichment in high field strength elements (HFSE) as well as in Rb, Th and HREE (data in Trua et al. 1999) and has an heterogeneous texture. This is reminiscent of the enrichment in HFSE and HREE in highly evolved granitic liquids, resulting from their increased solubilities in residual melts in presence of F (e.g. Keppler 1993). Increasing F content in a granitic melt reduces the partitioning of Cl to the fluid with drastic effect on fluid-melt partition coefficients of Cl-complexed elements such as Rb or Sr (e.g. Bai and Van Groos 1999; Audétat et al. 2000). Furthermore, fluid immiscibility may affect the evolution of volatile-rich magmatic systems at the magmatic-hydrothermal transition, and is enhanced in peralkaline compositions and in the presence of nonsilicate anions such as F and Cl (e.g. Veksler 2004). In particular, the partition coefficients of Ca between silicate and hydrosaline (F-bearing) melts is three orders of magnitude higher than those of K (e.g. Veksler 2004). Because of the similar properties of Sr and Rb with those of Ca and K, respectively, the same kind of differential fractionation is expected between these elements. All these data suggest that the halogen-rich fluids identified in the late stage evolution of peralkaline MER rhyolites may have played a significant role in the generation of their strong Sr isotope heterogeneity. Complex fractionation processes between Rb and Sr may occur in the magmas themselves because of these fluids but it is also probable that they have some effect on the destabilisation/melting processes affecting the close country rocks. Rb or ^{87}Sr released during biotite breakdown could be much more easily transported into the magma with such fluids than by selective crustal contamination. Such pervasive fluid interactions affecting Sr isotopes but not Nd and Pb isotopes would account for the association of uncontaminated and contaminated signatures at a small-scale in a single sample.

Acknowledgements F. Vidal and Ch. Bosq are thanked for their help with the chemical preparation of some samples and the Rb measurements. I am grateful to A. Gourgaud and especially Ch. Pin for fruitful discussions, comments and suggestions on various versions of the manuscript. J. Simon and an anonymous reviewer are thanked for their careful and insightful reviews. The detailed comments and suggestions of the associate editor (M.A. Clynne) greatly helped to improve this paper.

References

Abebe B, Boccaletti M, Bonini M, Mazzuoli R, Piccardi L, Tortorici L, Trua T (1997) Geological map of Asela region. S.E.L.C.A., Firenze

Annen C, Sparks RSJ (2002) Effects of repetitive emplacement of basaltic intrusions on thermal evolution and melt generation in the crust. Earth Planet Sci Lett 203:937–955 doi:10.1093/petrology/egi084

Audétat A, Günther D, Heinrich CA (2000) Magmatic-hydrothermal evolution in a fractionating granite: a microchemical study of the Sn–W–F–mineralized Mole granite (Australia). Geochim Cosmochim Acta 64:3373–3393 doi:1016/S0016-7037(00)00428-2

Bai TB, Van Groos K (1999) The distribution of Na, K, Rb, Sr, Al, Ge, Cu, W, Mo, La, and Ce between granitic melts and coexisting aqueous fluids. Geochim Cosmochim Acta 63:1117–1131 doi:10.1016/S0016-7037(98)00284-1

Baker BH, Henage LF (1977) Compositional changes during crystallization of some peralkaline silicic lavas of the Kenya rift valley. J Volcanol Geotherm Res 2:17–28 doi:10.1016/0377-0273(77)90013-0

Birck JL (1986) Precision K–Rb–Sr isotopic analysis: application to Rb–Sr chronology. Chem Geol 56:73–83 doi:10.1016/0009-2541(86)90111-7

Boccaletti M, Getaneh A, Mazzuoli R, Tortorici L, Trua T (1995) Chemical variations in a bimodal magma system: the Plio-Quaternary volcanism in the Dera Nazret area (Main Ethiopian Rift, Ethiopia). Africa Geosci Rev 2:37–60

Bohrson WA, Reid MR (1997) Genesis of silicic peralkaline volcanic rocks in an ocean island setting by crustal melting and open-system processes: Socorro Island, Mexico. J Petrol 38:1137–1166

Caricchi L, Ulmer P, Peccerillo A (2006) A high-pressure experimental study on the evolution of the silicic magmatism of the Main Ethiopian Rift. Lithos 91:46–58 doi:10.1016/j.lithos.2006.03.008

Charlier BLA, Ginibre C, Morgan D, Nowell GM, Pearson DG, Davidson J, Ottley CJ (2006) Methods for the microsampling and high-precision analysis of strontium and rubidium isotopes at single crystal scale for petrological and geochronological applications. Chem Geol 232:114–133 doi:10.1016/j.chemgeo.2006.02.015

Chernet T, Travi Y, Valles V, Gibert E (1997) The occurrence and hydrogeochemistry of fluoride in natural waters in the Ethiopian Rift. In: Abstracts of the International Symposium: Flood Basalts, Rifting and Paleoclimates in the Ethiopian Rift and Afar Depression. Addis Ababa, Ethiopia, pp 21–22 February 3–14, 1997

Christensen JN, DePaolo DJ (1993) Time scales of large volume silicic magma systems: Sr isotopic systematics of phenocrysts and glass from the Bishop Tuff, Long Valley, California. Contrib Mineral Petrol 113:100–114 doi:10.1007/BF00320834

Christensen JN, Halliday AN, Lee D-C, Hall CM (1995) In situ Sr isotopic analysis by laser ablation. Earth Planet Sci Lett 136:79–85 doi:10.1016/0012-821X(95)00181-6

Davidson J, Wilson IR (1989) Evolution of an alkali basalt-trachyte suite from Jebel Marra volcano, Sudan, through assimilation and fractional crystallization. Earth Planet Sci Lett 95:141–160 doi:10.1016/0012-821X(89)90173-8

Davidson J, Tepley FJ III (1997) Recharge in volcanic systems: evidence from isotope profiles of phenocrysts. Science 275:826–829 doi:10.1126/science.275.5301.826

Davidson J, Hora JM, Garrison JM, Dungan MA (2005) Crustal forensics in arc magmas. J Volcanol Geotherm Res 140:157–170 doi:10.1016/j.jvolgeores.2004.07.019

Davies GR, MacDonald R (1987) Crustal influences in the petrogenesis of the Naivasha basalt–comendite complex: combined trace element and Sr–Nd–Pb isotope constraints. J Petrol 28:1009–1031

Deniel C, Pin C (2001) Single-stage method for the simultaneous isolation of lead and strontium from silicate samples for isotopic measurements. Anal Chim Acta 426:95–103

Deniel C, Vidal Ph, Coulon C, Vellutini PJ, Piguet P (1994) Temporal evolution of mantle sources during continental rifting: the volcanism of Djibouti (Afar). J Geophys Res 99:2853–2869

Deniel C, Aydar E, Gourgaud A (1998) The Hasan Dagi stratovolcano (Central Anatolia, Turkey): evolution from calc-alkaline to alkaline magmatism in a collision zone. J Volcanol Geotherm Res 87:275–302

Deniel C, Trua T, Mazzuoli R (2000) Crustal control in the genesis of Plio-Quaternary bimodal magmatism of the Main Ethiopian Rift (MER): geochemical and isotopic (Sr, Nd, Pb) evidence—reply. Chem Geol 168:5–7 doi:10.1016/S0009-2541(00)00183-2

Duffield WA, Ruiz J (1992) Compositional gradients in large reservoirs of silicic magma as evidenced by ignimbrites versus Taylor Creek rhyolite lava domes. Contrib Mineral Petrol 110:192–210 doi:10.1007/BF00310738

Duffield WA, Ruiz J (1998) A model to explain Sr-isotope disequilibrium between feldspar phenocrysts and melt in large-volume silicic magma systems. J Volcanol Geotherm Res 87:7–13 doi:10.1016/S0377-0273(98)00071-7

Duffield WA, Ruiz J, Webster JD (1995) Roof–rock contamination of magma along the top of the reservoir for the Bishop Tuff. J Volcanol Geotherm Res 69:187–195 doi:10.1016/0377-0273(95)00026-7

Futa K, Hedge CE, Hearn BC Jr, Donnelly-Nolan JM (1981) Strontium isotopes in the Clear Lake volcanics. US Geol Surv Prof Pap 1141:61–66

Gardner JE, Sigurdsson H, Carey SN (1991) Eruption dynamics and magma withdrawal during the Plinian phase of the Bishop Tuff eruption, Long Valley Caldera. J Geophys Res 96:8097–8111

Gioncada A, Mazzuoli R, Bisson M, Pareschi MT (2003) Petrology of volcanic products younger than 42 ka on the Lipari–Vulcano complex (Aeolian islands, Italy): an example of volcanism controlled by tectonics. J Volcanol Geotherm Res 122:191–220 doi:10.1016/S0377-0273(02)00502-4

Halliday AN, Fallick AE, Hutchinson J, Hildreth W (1984) A Nd, Sr and O isotopic investigation into the causes of chemical and isotopic zonation in the Bishop Tuff, California. Earth Planet Sci Lett 68:379–391 doi:10.1016/0012-821(84)90123-7

Halliday AN, Mahood GA, Holden P, Metz JM, Dempster TJ, Davidson JP (1989) Evidence for long residence times of rhyolitic magma in the Long Valley magmatic system: the isotopic record in precaldera lavas of Glass Mountain. Earth Planet Sci Lett 94:274–290 doi:10.1016/0012-821(89)90146-5

Heumann A, Davies GR (2002) U–Th disequilibrium and Rb–Sr age constraints on the magmatic evolution of peralkaline rhyolites from Kenya. J Petrol 43:557–577

Heumann A, Davies GR, Elliott T (2002) Crystallization history of rhyolites at Long Valley, California, inferred from combined U-series and Rb–Sr isotope systematics. Geochim Cosmochim Acta 66:1821–1837 doi:10.1016/S0016-7037(01)00883-3

Hildreth W, Halliday A, Christiansen RL (1991) Isotopic and chemical evidence concerning the genesis and contamination of basaltic and rhyolitic magma beneath the Yellowstone Plateau volcanic field. J Petrol 32:63–138

Karapetian SG, Jrbashian RT, Mnatsakanian AKh (2001) Late collision rhyolitic volcanism in the north-eastern part of the Armenian Highland. J Volcanol Geotherm Res 112:189–220 doi:10.1016/S0377-0273(01)00241-4

Keppler H (1993) Influence of fluorine on the enrichment of high field strength trace elements in granitic rocks. Contrib Mineral Petrol 114:479–488 doi:10.1007/BF00321752

Knesel KM, Davidson J, Duffield WA (1999) Evolution of silicic magma through assimilation and subsequent recharge: evidence from Sr isotopes in sanidine phenocrysts, Taylor Creek rhyolite, NM. J Petrol 40:773–786

Lu F, Anderson AT, Davis AM (1992) Melt inclusions and crystal–liquid separation in rhyolitic magma of the Bishop Tuff. Contrib Mineral Petrol 110:113–120 doi:10.1007/BF00310885

Mahatsente R, Jentzsch G, Jahr T (1999) Crustal structure of the Main Ethiopian Rift from gravity data: 3-dimensional modeling. Tectonophysics 313:363–382 doi:10.1016/S0040-1951(99)00213-9

McCulloch MT, Kyser TK, Woodhead JD, Kinsley L (1994) Pb–Sr–Nd–O isotopic constraints on the origin of rhyolites from the Taupo Volcanic Zone of New Zealand: evidence for assimilation followed by fractionation from basalt. Contrib Mineral Petrol 115:303–312 doi:10.1007/BF00310769

Mohr P (1992) Nature of the crust beneath magmatically active continental rifts. Tectonophysics 213:269–284 doi:10.1016/0040-1951(92)90263-6

Mohr P, Zanettin B (1988) The Ethiopian flood basalt province. In: MacDougall JD (ed) Continental flood basalts. Kluwer, Dordrecht, pp 63–110

Noble DC (1967) Sodium, potassium and ferrous iron contents of some secondarily hydrated natural silicic glasses. Am Mineral 52:280–286

Noble DC, Hedge CE (1969) $^{87}Sr/^{86}Sr$ variations within individual ash-flow sheets. US Geol Surv Prof Paper 650-C:133–139

Pankhurst RJ, O'Nions K (1973) Determination of Rb/Sr and $^{87}Sr/^{86}Sr$ ratios of some standard rocks and evaluation of X-Ray fluorescence spectrometry in Rb–Sr geochemistry. Chem Geol 12:127–136 doi:10.1016/0009-2541(73)90110-1

Paquereau Lebti P, Thouret JC, Wörner G, Fornari M (2006) Neogene and Quaternary ignimbrites in the area of Arequipa, Southern Peru: stratigraphical and petrological correlations. J Volcanol Geotherm Res 154:251–275 doi:10.1016/j.jvolgeores.2006.02.014

Petford N, Gallagher K (2001) Partial melting of mafic (amphibolitic) lower crust by periodic influx of basaltic magma. Earth and Planet Sci Lett 193:483–499 doi:10.1016/S0012-821X(01)00481-2

Pin C, Bassin Ch (1992) Evaluation of a strontium-specific extraction chromatographic method for isotopic analysis in geological materials. Anal Chim Acta 269:249–255

Pin C, Briot D, Bassin Ch, Poitrasson F (1994) Concomitant separation of strontium and samarium–neodymium for isotopic analysis in silicate samples, based on specific extraction chromatography. Anal Chim Acta 298:209–217

Pin C, Joannon S, Bosq Ch, Le Fèvre B, Gauthier PJ (2003) Precise determination of Rb, Sr, Ba, and Pb in geological materials by isotope dilution and ICP-quadrupole mass spectrometry following separation of the analytes. J Anal At Spectrom 18:135–141 doi:10.1039/b211832g

Reece C, Ruiz J, Duffield WA, Patchett PJ (1990) Origin of Taylor Creek rhyolite magma, Black Range, New Mexico, based on Nd–Sr isotope studies. Geol Soc Am Bull Spec Pap 246:263–273

Schmitz MD, Smith IEM (2004) The petrology of the Rotoiti eruption sequence, Taupo volcanic zone: an example of fractionation and mixing in a rhyolitic system. J Petrol 45:2045–2066 doi:10.1093/petrology/egh047

Snyder DC, Widom E, Pietruszka AJ, Carlson RW (2004) The role of open-system processes in the development of silicic magma chambers: a chemical and isotopic investigation of the Fogo A trachyte deposit, Sao Miguel, Azores. J Petrol 45:723–738

Stix J, Gorton MP (1990) Variations in trace element partition coefficients in sanidine in the Cerro Toledo rhyolite, Jemez Mountains, New Mexico: effects of composition, temperature, volatiles. Geochim Cosmochim Acta 54:2697–2708 doi:10.1016/0016-7037(90)90005-6

Stuckless JS, O'Neil JR (1973) Petrogenesis of the Supertition–Superior volcanic area as inferred from strontium- and oxygen-isotope studies. Geol Soc Am Bull 84:1987–1998

Tepley FJ III, Davidson J, Clynne MA (1999) Magmatic interactions as recorded in plagioclase phenocrysts of Chaos Crags, Lassen volcanic center, California. J Petrol 40:787–806

Tepley FJ III, Davidson J, Tilling RI, Arth JG (2000) Magma mixing, recharge and eruption histories recorded in plagioclase phenocrysts from El Chichon volcano, Mexico. J Petrol 41: 1397–1411

Trua T, Deniel C, Mazzuoli R (1999) Crustal control in the genesis of Plio-Quaternary bimodal magmatism of the Main Ethiopian Rift (MER): geochemical and isotopic (Sr, Nd, Pb) evidence. Chem Geol 155:201–231 doi:10.1016/S0009-2541(98)00174-0

Vasquez JA, Reid MR (2002) Time scales of magma storage and differentiation of voluminous high-silica rhyolites at Yellowstone caldera, Wyoming. Contrib Mineral Petrol 144:274–285 doi:10.1007/s00410-002-0400-7

Veksler IV (2004) Liquid immiscibility and its role at the magmatic-hydrothermal transition: a summary of experimental studies. Chem Geol 210:7–31 doi:10.1016/j.chemgeo.2004. 06.002

Vidal Ph, Bernard-Griffiths J, Cocherie A, Le Fort P, Peucat JJ, Sheppard SMF (1984) Geochemical comparison between Himalayan and Hercynian leucogranites. Phys Earth Planet Int 35:179–190 doi:10.1016/0031-9201(84)90041-4

Weaver SD, Gibson IL, Houghton BF, Wilson CJN (1990) Mobility of rare earth and other elements during crystallization of peralkaline silicic lavas. J Volcanol Geotherm Res 43:57–70 doi:10.1016/0377-0273(90)90044-G

WoldeGabriel G, Aronson JL, Walter RC (1990) Geology, geochronology and rift basin development in the central sector of the Main Ethiopian Rift. Geol Soc Am Bull 102:439–458 doi:10.1130/0016-7606(1990)102<0439:GGARBD>2.3.CO;2

Wolff JA, Ramos FC, Davidson J (1999) Sr isotope disequilibrium during differentiation of the Bandelier Tuff: constraints on the crystallization of a large rhyolitic magma chamber. Geology 27:495–498